



Purifying Effect Evaluation of Pavement Surfacing Materials Modified by Novel Modifying Agent

Xiaolong Sun^{1*}, Zhisheng Liu², Xiao Qin³, Dongfang Zeng¹ and Yingmei Yin¹

¹ School of Civil and Transportation Engineering, Guangdong University of Technology, Guangzhou, China, ² The Key Laboratory of Road and Traffic Engineering, Ministry of Education, Tongji University, Shanghai, China, ³ School of Transportation and Civil Engineering and Architecture, Foshan University, Foshan, China

Functional pavement material with an exhaust-purifying performance has gradually become of greater interest to researchers in recent years. For improving the purifying effect of functional micro surfacing, two types of raw ore powders with exhaust-purifying potentials were selected as novel functional modifiers. Firstly, the road performance of purifying micro surfacing was evaluated according to the ASTM and ISSA standards. Then, the dispersion state of modifying agents in emulsified asphalt evaporation residue was analyzed and discussed using SEM and FTIR. Finally, the purifying effect of micro surfacing on exhausts was examined in a laboratory to investigate the impact of various experimental conditions on the purifying performance. Meanwhile, the purifying performance was also monitored in a field test. The results showed that the road performance of purifying micro surfacing could fulfill the requirements of relevant technical standards. Pyrite had better dispersion property than specularite and titanium dioxide inside asphalt. The purifying micro surfacing could achieve a better purifying effect on NO_x and CO_x than traditional micro surfacing with TiO₂. These environmentally friendly pavement materials could provide new solutions for the reduction of polluting emissions in automobile exhausts.

Keywords: pavement, micro surfacing, exhaust purification, road performance, characterization

OPEN ACCESS

Edited by:

Jian Ouyang,
Dalian University of Technology, China

Reviewed by:

Cesare Sangiorgi,
University of Bologna, Italy
Huayang Yu,
South China University of
Technology, China

*Correspondence:

Xiaolong Sun
XLS1998@gdut.edu.cn

Specialty section:

This article was submitted to
Structural Materials,
a section of the journal
Frontiers in Materials

Received: 21 February 2020

Accepted: 15 May 2020

Published: 28 July 2020

Citation:

Sun X, Liu Z, Qin X, Zeng D and Yin Y
(2020) Purifying Effect Evaluation of
Pavement Surfacing Materials
Modified by Novel Modifying Agent.
Front. Mater. 7:180.
doi: 10.3389/fmats.2020.00180

INTRODUCTION

Road traffic an integral part of the existing transportation system. In 2019, the number of automobiles around the world had almost exceeded 1.39 billion. Even though various innovative solutions have been found and applied in the automobile industry, the share of internal combustion engine vehicles (including hybrid vehicles) will remain prevalent for the next several decades (Wei et al., 2009; Miyamoto et al., 2012; Hirata, 2014), and thus the exhaust emissions will be one of the main atmospheric pollution sources (Rêgo et al., 2014). Due to incomplete combustion of hydrocarbon fuel in internal combustion engines, automobile exhausts including carbon monoxide (CO), hydrocarbons (HC), nitrogen oxides (NO_x), sulfur dioxides (SO₂), particulate matter (such as lead compounds, carbon black particles, or oil mist, etc.), and other atmospheric pollutants not only damage the natural environment, but also result in the haze pollution and urban heat island (UHI) effect (Çay et al., 2013; Fattah et al., 2013; Pinzi et al., 2013; Labarraque et al., 2015; Peng et al., 2015). Meanwhile, the emission increases of NO_x, SO₂, and particulate matter also increase the risk of cancer in humans (Tong et al., 2014). Therefore, the control of automobile exhausts is vital to protecting the environment and human health from air pollution.

Currently, the most common methods used to reduce exhaust emissions include the control of pollution sources, improvement of air exchange, development of new energy sources, and application of exhaust purifiers (Brijesh and Sreedhara, 2013; Amato et al., 2014; Beale et al., 2015). However, due to the large number of vehicles, the effectiveness of these solutions for emission reduction is limited (Yan et al., 2014; Goel and Guttikunda, 2015; Yu et al., 2017, 2019, 2020). Improving air exchange could lower the pollutant concentration within specific territories, but this method could hardly reduce the total amount of pollutant emissions. In recent years, the application of new energy sources has been widely researched as an indirect method to mitigate exhaust pollution (Kimble and Wang, 2013; Liu and Liang, 2013; Habib and Wenzel, 2014). As a result, the number of electric and fuel cell vehicles increases gradually (Hwang, 2013; Jhala et al., 2014). However, the share of internal combustion engine vehicles will remain prevalent for the next few decades (Sprouse and Depcik, 2013; Wang et al., 2013). At present, the use of exhaust purifiers has been proven to be the most efficient way to purify the pollution from exhaust gases. The existing exhaust purifiers are mainly divided into three types: one-stage catalyst, two-stage catalyst, and three-way catalyst (Schmeisser et al., 2013; Hofmann et al., 2015). Among these exhaust purifiers, three-way catalyst is the most popular and efficient exhaust purifier, which can effectively transform CO, HC, and NO_x into harmless gas (Opitz et al., 2014; Lan et al., 2015; Zeng and Hohn, 2016). However, there are still some disadvantages of the three-way catalyst, such as its low conversion rate under lean-burn, poor durability of purifying effect, and soot particle contamination, which makes it difficult to meet the ever-growing needs of the atmospheric environment protection (Park et al., 2015). In addition, the existing methods could only purify pollutants before emitting into the air, but not reduce the pollution gas already emitted to the atmosphere. Therefore, it is important to develop an effective way to purify both the exhaust gas emitted from vehicles and those into the atmosphere.

Pavement, as a road traffic carrier, has a huge contact area with the atmospheric environment. If the exhaust purifying effect could be achieved on pavement material, the exhausts emitted from vehicles might be controlled effectively within specific airspaces and converted into harmless gas. Micro surfacing was one of the most effective ways for quick maintenance of pavements (Ouyang et al., 2016, 2018a,b, 2019; Qin et al., 2018). The thickness, material composition, and quick construction promote the feasibility of applying micro surfacing for achieving the purifying function of pavement (Sun et al., 2018, 2020a,b; Chen et al., 2020; Wang et al., 2020). Therefore, in this paper, two novel functional materials with exhaust-purifying potentials were obtained from raw ore powders and modified with two auxiliary modifiers. The applying feasibility of novel modifying agents was evaluated through road performance and micro characterization. Furthermore, the impacts of various influencing factors on purifying performances of the new hybrid micro surfacing material were investigated by laboratory and field test. This study provides scientific references for further study of functional pavement materials.

TABLE 1 | Technical properties of selected functional materials.

Composition information	Fineness (Mesh)	Density (g·cm ³)	Main ingredient content (%)
Rutile titanium dioxide	3,000	4.26	98
Pyrite	325	4.9	90
Specularite	325	4.7	92

TABLE 2 | Technical properties of selected surface modifiers.

Modifying agent	Boiling point/°C	Flash point/°C	Relative density (25°C)	Molecular weight
Isopropanol	82.3	12	0.79	60.06
Silane coupling agent (KH-550)	217	135	1.04	221.4

MATERIALS AND PREPARATION

Materials

Functional Materials

Considering the purification potential and compatibility between modifiers and asphalt, pyrite, specularite, and titanium dioxide were selected as the functional materials for this study, which were named as P, S, and TD for short in this paper, respectively. Technical performances of purifying functional materials are shown in **Table 1**.

The purifying functional materials contained two types of combinations, rutile titanium dioxide and pyrite, and rutile titanium dioxide and specularite, named as PTD and STD, respectively. The weight ratio of rutile titanium dioxide to pyrite or specularite was 1:1. Pyrite and specularite were obtained from raw ore powders, which might have adverse effects on the compatibility with asphalt. Therefore, isopropanol and a silane coupling agent were used to improve the surface property and enhance the purifying performance (Liu et al., 2019a,b). The technical properties of selected modifiers are shown in **Table 2**.

Modified Emulsified Asphalt

Styrene Butadiene Rubber (SBR) modified emulsified asphalt was used as a binder in this study. The content of SBR modified emulsified asphalt was 12.6% by dry weight of aggregate. The technical properties of SBR modified emulsified asphalt are detailed in **Table 3**.

Aggregate, Water, and Additive

Basalt was chosen as the aggregate and the sand equivalent value was 72%, which could reach the limit value of (ASTM D2419, 2014; Huang et al., 2020). The water used for micro surfacing was free of oil contamination. The salinity was below 5,000 mg/L. Specifically, the sulfate content was below 2,700 mg/L. Furthermore, the PH of the water was below 6. The content of water was 8.4% by dry weight of aggregate. In order to control the demulsification of SBR emulsified asphalt, this paper selected ordinary Portland cement as an additive to prepare

micro surfacing. Its content was $\sim 2\%$ by dry weight of aggregate (Ouyang et al., 2020).

Modification of Purifying Functional Materials

The modification of functional materials mainly includes the following procedures (detailed in Figure 1):

(a) Sieve the functional materials: Pyrite and specularite were carefully washed with distilled water to remove dust and impurities, and dried at 110°C for 5 h in a pre-heated oven. Then, pyrite and specularite were filtered through a 0.044 mm sieve. The treated powder was placed into a clean container.

(b) Mill functional material: In order to increase the specific surface area and improve catalytic potential, pyrite, and specularite powder were subjected to high-energy ball milling under the protection of ethanol and inert gas.

(c) Perform surface modification: Silane coupling agent, isopropanol, and water were mixed to prepare the chemical solution, whose mass ratio was $\sim 20:72:8$. The solution was subsequently treated by ultrasonic dispersion apparatus for 10 min. Then, pyrite and specularite were added into the solution, and the mixture was stirred at the speed of $5,000\text{ rad/min}$ for 15 min. Finally, the mixture was kept still for 1 h, and then the modified pyrite and specularite were filtered into a clean beaker.

(d) Conduct vacuum drying: The beaker containing pyrite and specularite were put into an 80°C vacuum drying oven for 5 h. The drying process was conducted in an inert gas atmosphere to ensure the chemical stability of pyrite and specularite.

TABLE 3 | Technical properties of SBR modified emulsified asphalt.

Test	Value	Specification	Test method
Penetration of emulsified asphalt residue (25°C , 100 g, 5 s) (0.1 mm)	76	40–90	ASTM D5, 2013
Ductility of emulsified asphalt residue (5°C) (cm)	58	>20	ASTM D113, 2007
Distillation of emulsified asphalt (%)	63.3	≥ 62	ASTM D6997, 2004
Storage of emulsified asphalt (1 d) (%)	0.04	≤ 1	ASTM D6930, 2010
Residue on sieve (1.18 mm) (%)	0.03	≤ 0.1	ASTM D244, 2017
Softening point of emulsified asphalt residue ($^\circ\text{C}$)	64	>57	ASTM D36, 2014

Testing Specimen Preparation

The designed gradation and mix proportion are shown in Table 4. The detailed preparation procedures (Figure 2) are shown as follows:

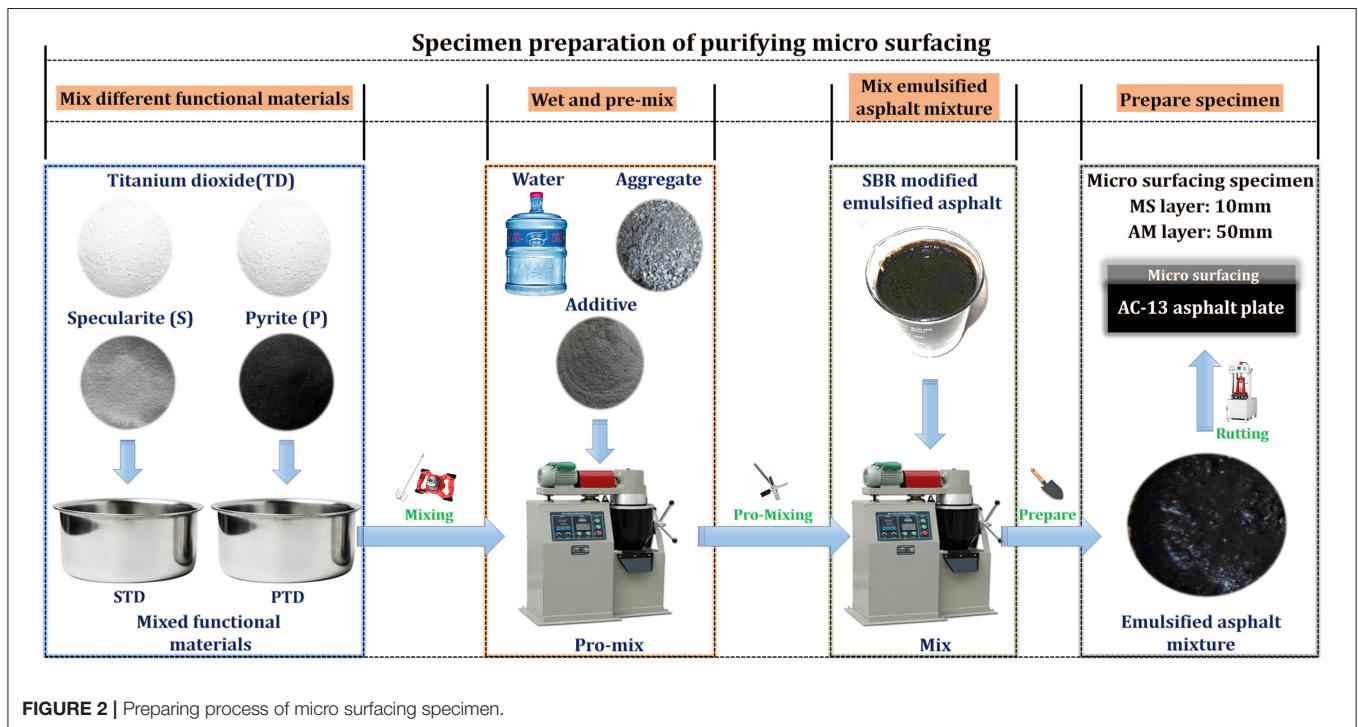
(a) Prepare emulsified asphalt mixture: Basalt aggregate, additive, and water were mixed for 5 min to ensure that the aggregate was wetted to prevent the early demulsification of the modified emulsified asphalt. Then the functional materials



TABLE 4 | Designed gradation and mix proportion of micro surfacing.

Gradation	Passing percentage (%)							
	9.5 mm	4.75 mm	2.36 mm	1.18 mm	0.6 mm	0.3 mm	0.15 mm	0.075 mm
Design gradation	100	80	57	39	27	17	11	8
ISSA A143	100	70–90	45–70	28–50	19–34	12–25	7–18	5–15
Component	Basalt aggregate	Emulsified asphalt	Functional material	Water	Additive			
Proportion (%)	100	12.6	6	8.4	2			

ISSA A143 Standard: "Recommend Performance Guideline for Micro Surfacing".

**FIGURE 2** | Preparing process of micro surfacing specimen.

were added into the wet mixture and mixed for 4 min. SBR modified emulsified asphalt was added into the mixing pot steadily and then the mixture was mixed for 3 min.

(c) **Prepare specimens for different tests:** For the purifying test, British pendulum slip test, and permeability test, the micro surfacing (30*30*1 cm) was paved on the rutting specimen of the asphalt mixture (AC-13, 30*30*5 cm) and preserved at $25 \pm 5^\circ\text{C}$. For the wet-track abrasion loss test and lateral displacement test, the prepared mixture was sampled, and cast in the molds on the surface of tar felt (Circular specimen 63.5 mm in diameter and rectangular specimen with the dimension of $38 \times 5 \times 0.6$ cm) and preserved at 60°C for 16 h.

TESTING METHOD

Road Performance

The British pendulum slip test, wet-track abrasion loss test, rutting test, and permeability test were conducted to assess the road performances of purifying micro-surfacing according to the

Standard ISSA TB-147, 2000; ASTM ED3910, 2011; ASTM E303, 2013, and JTG E60, 2008.

Micro Characterization

Scanning Electronic Microscopy Analysis (SEM)

Asphalt samples were prepared using the evaporation residue of purifying modified emulsified asphalt. The micro-morphology and particle size of functional materials in asphalt samples were characterized by SEM to determine the dispersion of functional materials inside asphalt. Then, the element composition of micro zones was statistically analyzed. The magnifications of the SEM test were 2,000, 4,000, and 10,000 times (Huang et al., 2019; Cai et al., 2020).

Fourier Transform Infrared Analysis (FTIR)

The FTIR analysis technology was used to investigate the characteristic peaks and functional groups of the evaporation residue with purifying modifiers. The wavenumber range of FTIR was from $4,000$ to 500 cm^{-1} . The weight of the sample was about $5\text{ }\mu\text{g}$.

Purifying Effect Evaluation Measurement System

The purifying effect measurement device, as shown in **Figure 3**, was developed according to ISO 7996 (1985), ISO 4224 (2000), ISO 10498 (2004), ISO 22197-1 (2007), which consisted of a temperature controlling system, data acquisition system, atmospheric pressure, and solar radiation controlling system. This device was used to investigate the purifying effect of purifying micro surfacing. The technical parameters were shown as follows: Temperature control range: -20 – 120°C , UV intensity range: 0 – 20 W/m^2 , Pressure tolerance range: 0 – 3 atm, and Gas concentration measurement range: 0.0 – 20.0 % vol (CO_x), 0 – $5,000 \times 10^{-6}$ vol (NO_x).

Laboratory Testing Condition and Procedure

The atmospheric pressure, specimen temperature, UV light source intensity, and pollutant concentration were chosen as the influencing variables of the purifying experiment. A used motorcycle engine was used as the supply unit of exhaust, whose pollutant concentrations could reach the ISO Standard concentration range. According to the parameter values of real pavement environment, various experiment conditions are designed for a purifying effect test, as shown in **Table 5**.

The laboratory test procures is detailed as follows:

(a) **Achieve the vacuum status:** All the outlets of the experimental device, except the one connected to the vacuum pump, were closed and the vacuum pump was turned on to achieve the vacuum status of the reactor cell. When air pressure reached the vacuum, the vacuum pump was turned off and the outlet connected to the vacuum pump was closed.

(b) **Adjust the concentration of pollutant gas:** The exhaust supply unit was started and preheated. The outlet connected to the test facility was opened and the exhaust gas was conveyed into the reactor cell of the test equipment along with air at the flow rate of 3.0 L/min, when the content of pollutant gas of exhaust tends to be stable. When the air pressure and the concentration of pollutant gas reached the desired values, the exhaust supply unit and all the outlets of the experimental device were closed.

(c) **Control the experimental condition and record the data:** The temperature of the specimen was raised up to the target temperature using a temperature control system and the UV light intensity was kept around the desired value by the corporation of a light source control system and radiometer. Then the gas flow controller and circulation system were turned on to keep the exhaust distributed evenly in the reactor cell of the test equipment. The test data were monitored by the exhaust analyzer dynamically and recorded by the data acquisition automatically.

Field Testing Method

A field test was performed to measure the purifying effect in a natural environment. An experiment period of 10 days in August was selected to evaluate the purifying effect of micro surfacing, whose solar radiation intensities, atmospheric temperatures, and humidities were similar to those in the pavement environment. Before the start of the field test, the

specimen was assembled inside the test device, then moved to the outside terrace sufficiently far from the surrounding buildings to avoid the shadow effect. The exhaust supplied by the motorcycle engine was conveyed along with air into the reactor cell after passing through a gas-washing bottle. When the desired exhaust concentration and air pressure were achieved through the coordination of the adjustment system and concentration monitoring system, all the outlets of the gas supply unit and the experiment apparatus were closed. The pollutant concentration, solar radiation intensity, and specimen temperature were monitored per hour using the gas analyzer, radiometer, and temperature sensor. The field test device is shown in **Figure 3**.

RESULTS AND DISCUSSION

Road Performance

The results of road performances are shown in **Table 6**. It can be seen from **Table 6** that there were only slight differences in pavement performances between a purifying micro surfacing and a normal one, which indicated that the replacement of mineral filler by functional material would not lead to a negative effect on the pavement performances of micro surfacing, which lay a solid base for the application of PTD and STD materials in micro surfacing.

Dispersion and Fusion State Analysis SEM/EDS Analysis

The microscopic graphs of PTD and STD emulsified asphalt residue and net residue were taken to characterize the microstructure of functional materials in asphalt and evaluate the compatibility between functional material and asphalt. The SEM graphs of purifying emulsified asphalt residue are shown in **Figure 4**.

It can be seen from **Figure 4B** that the bright particles represented different micro shapes, and particle sizes were evenly dispersed in asphalt, which might indicate the productive dispersion of PTD in asphalt. Through particle sizing results, the particle size ranged from 3.1 to 10 μm and most of the identified particles were around 4 μm or smaller in size. **Figure 4C** demonstrated the micro distribution state of STD in asphalt. It could be observed from **Figure 4C** that the distribution of particle size was mainly concentrated in the range from 2 to 10 μm , similar to that of PTD. However, a few big bright particles could be identified at 10 K magnification, which suggested that the specularite might not be dispersed evenly in asphalt material. Meanwhile, the element composition of micro zone in the SEM graph was analyzed and the analysis results are shown in **Figure 5**.

It can be seen from **Figure 5** that Fe, S, and O elements, as typical elements, were identified obviously in most of the scanning zones. Ti was also characterized in the micro zone, but the identified number of micro zones was smaller than that of other elements, which was presented in **Figure 5** (VI). Ti was the typical element of titanium dioxide, which might reflect the dispersion state of titanium dioxide in micro surfacing.



FIGURE 3 | Laboratory and field test of exhaust purification performance.

TABLE 5 | Experimental condition of purifying effect measurement.

Impact factor	Variable values	Test time	Experimental conditions
Atmospheric pressure	0.6, 0.8, 1.0, 1.2, 1.4, 1.6 atm	5 h	Ambient temperature:25°C UV light intensity:10 W/m ² NO _x :60–70 ppm CO _x :70–80 ppm Humidity:50%
Specimen temperatures	30, 35, 40, 45, 50, 55, 60°C	5 h	UV light intensity:10 W/m ² Air pressure:1.0 atm NO _x :60–70 ppm CO _x :70–80 ppm Humidity:50%
UV light source intensity	4, 6, 8, 10, 12, 14 W/m ²	5 h	Air pressure:1.0 atm Ambient temperature:25°C NO _x :60–70 ppm CO _x :70–80 ppm Humidity:50%
Pollutant concentration	NO _x 40, 50, 60, 70, CO _x 80 ppm	5 h	Air pressure:1.0 atm Ambient temperature:25°C UV light intensity:10 W/m ² Humidity:50%
Field test	Ambient temperature, specimen temperatures, UV light intensity	8 h (Solar exposure time)	Air pressure:1.0 atm NO _x :60–70 ppm CO _x :70–80 ppm

The related ISO Standard of air purifying material that the test time should be no <5 h.

FTIR Analysis

The composition of functional groups was one of the most important parameters to indicate the chemical variation inside micro surfacing. Compared to the basic micro surfacing with no functional materials, the functional groups' variation of purifying micro surfacing was examined to explain the molecular structure after the addition of functional materials using the FTIR test. The FTIR analysis results are shown in **Figure 6**.

It can be seen from **Figure 6** that the transmission curves of purifying micro surfacing differed from that of the control group without functional materials. For PTD, the different transmission rates appeared in the wave number positions of 3,500, 1,750, 1,200, and 750 cm⁻¹. Regarding STD, the different

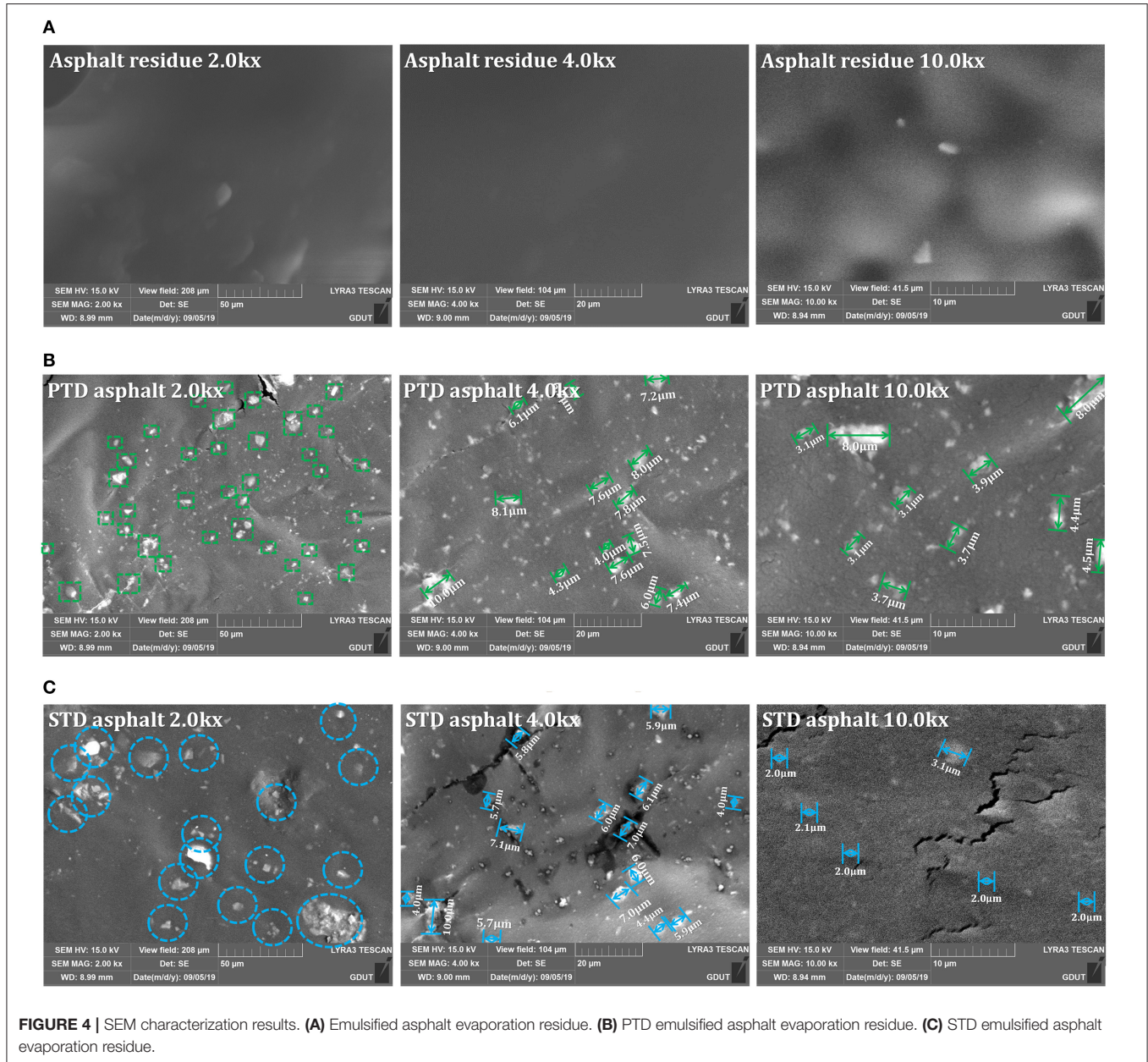
transmission rates arose in the wave number positions of 1,500 and 750 cm⁻¹. The change of transmission rate in certain wave numbers could indicate that the functional materials, pyrite, and specularite, might help improve the purifying effect of micro surfacing though the chemical modification led by chemical characteristics.

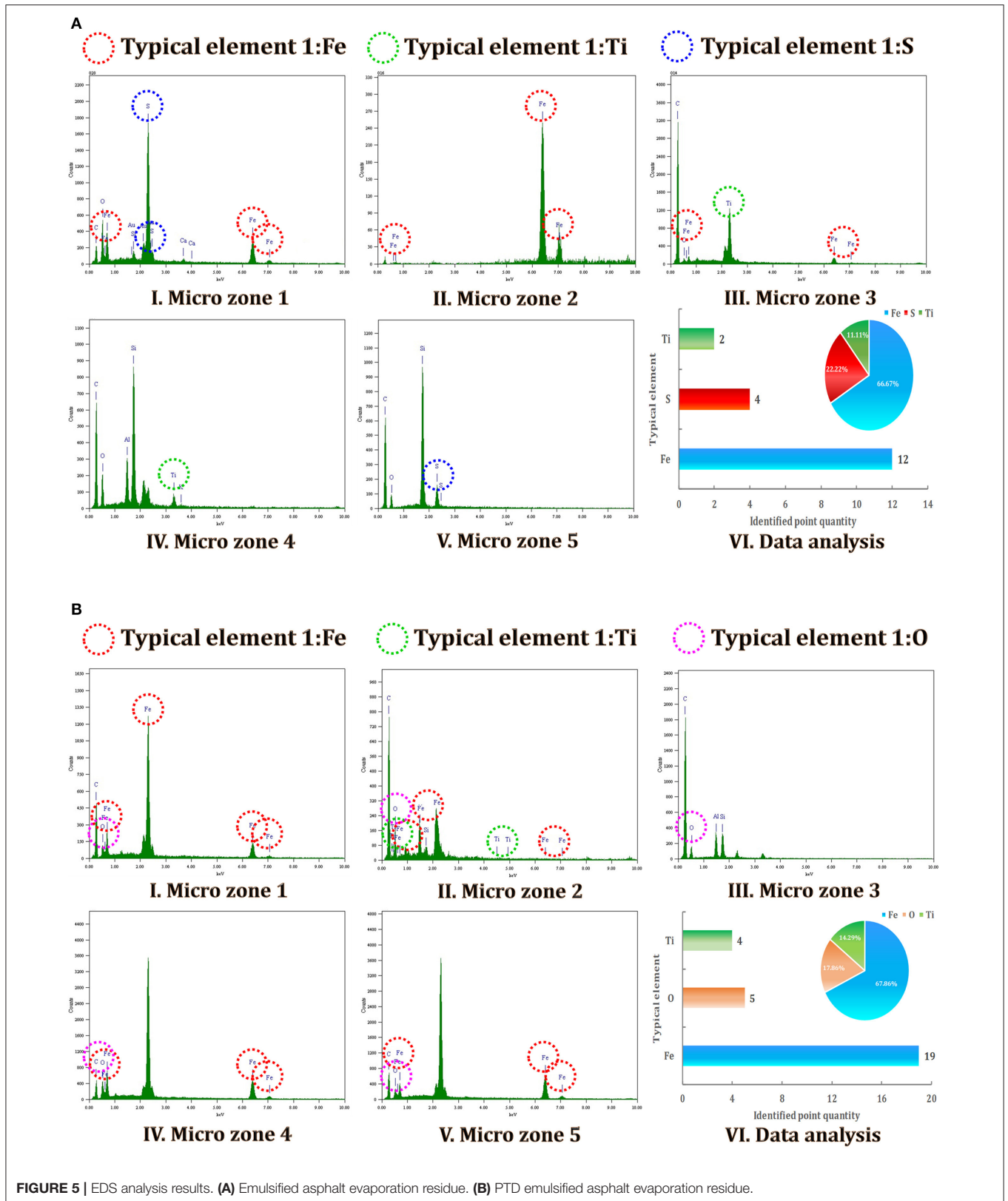
Laboratory Evaluation of Purifying Effect Air Pressure Condition

The impacts of atmospheric pressure on the purification effect was investigated in this section to guarantee the accuracy of the experiment. In **Figure 7A**, the results of the purifying test at different atmospheric pressures are presented. As the

TABLE 6 | Road performances of purifying micro surfacing and normal micro surfacing.

Test		PTD/STD micro surfacing	Normal micro surfacing	Standard requirements
British pendulum slip test (BPN)		74/77	75	≥45
Wet-track abrasion loss test	1 h Abrasion loss (g/m ²)	440.5/443.2	445.6	≤538
	6 d Abrasion loss (g/m ²)	605/606	609	≤807
Lateral displacement test	Lateral displacement (%)	3.0/3.1	3.1	≤5
	Relative density	1.61/1.60	1.63	≤2.10
Permeability test (ml/min)		7/7	7	10





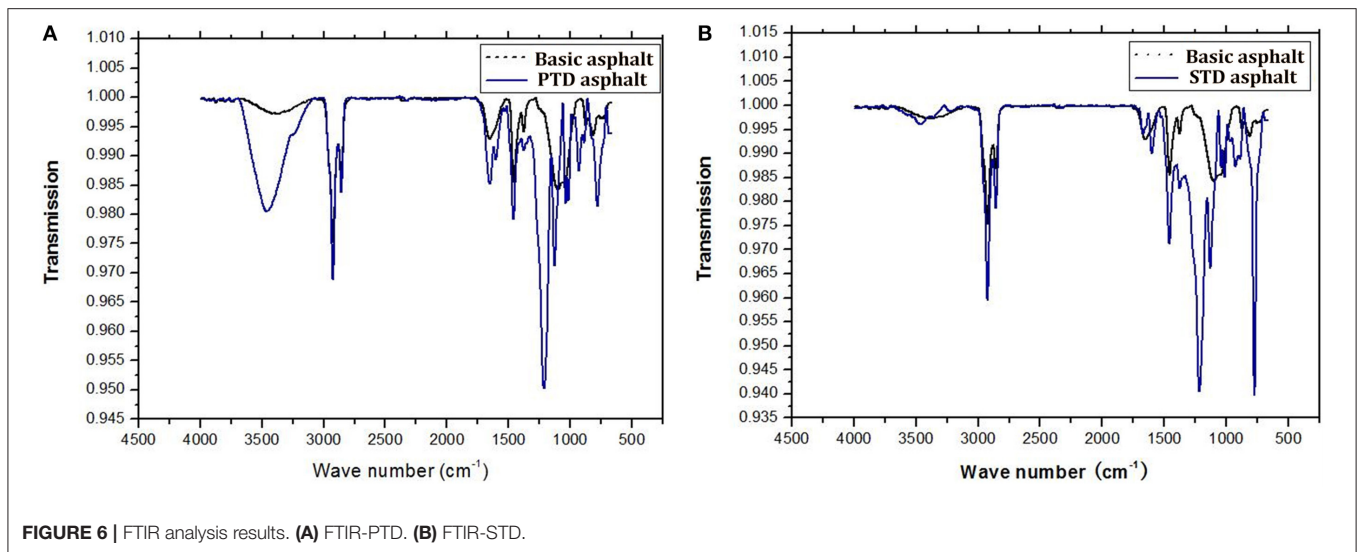


FIGURE 6 | FTIR analysis results. (A) FTIR-PTD. (B) FTIR-STD.

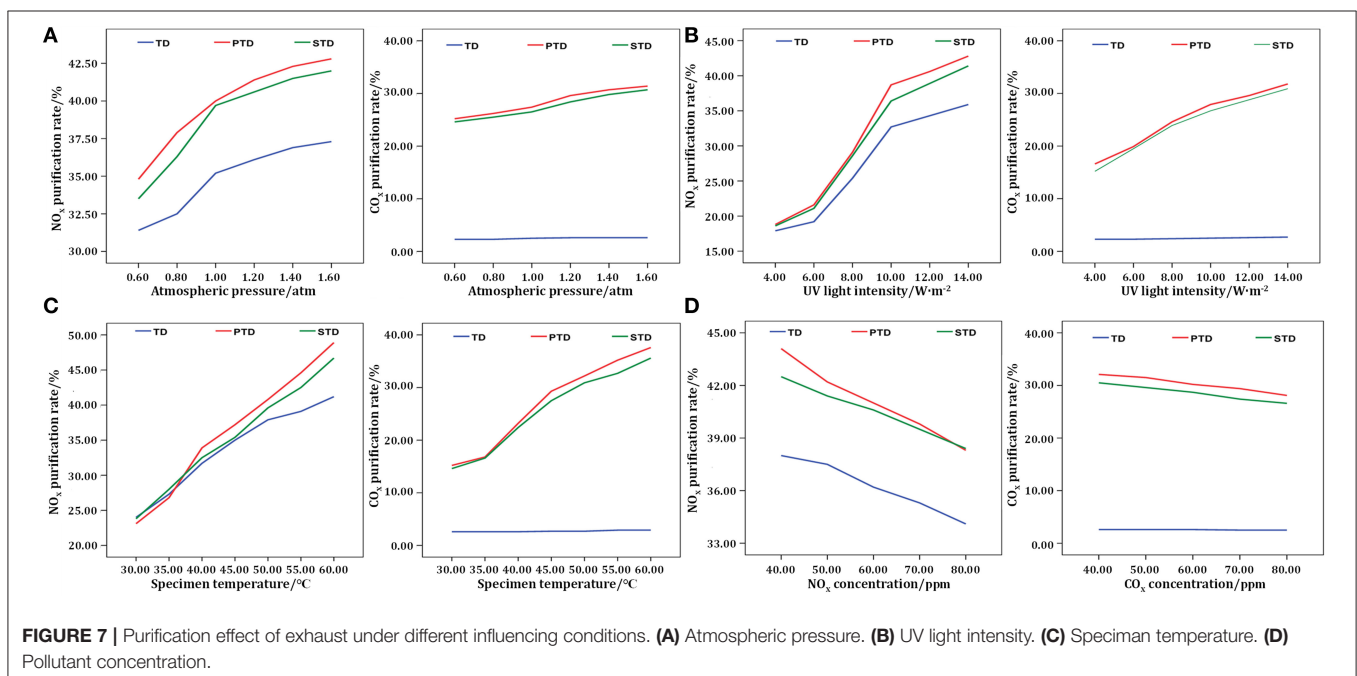


FIGURE 7 | Purification effect of exhaust under different influencing conditions. (A) Atmospheric pressure. (B) UV light intensity. (C) Specimen temperature. (D) Pollutant concentration.

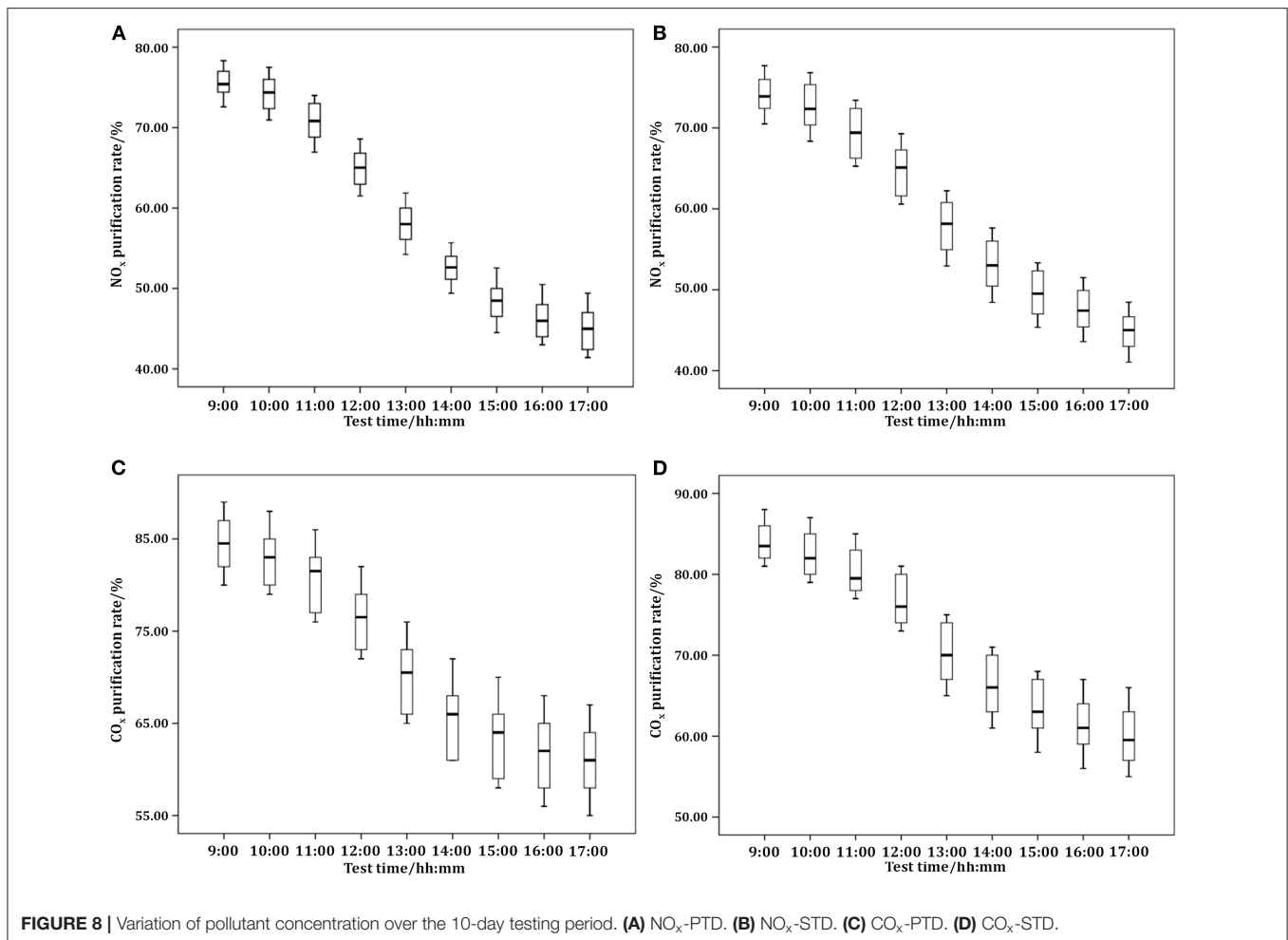
atmospheric pressure increased gradually, the purifying effect of micro surfacing on pollutants also showed an obviously increasing trend. Moreover, when the atmospheric pressure exceeded 1.0 atm, the increasing speed of the purifying effect began to slow down and tended to be stable. While the atmospheric pressure increased from 0.6 to 1.6 atm, the purifying effect of PTD and STD on NO_x rose to ~ 34 and 42%, respectively. Interestingly, PTD and STD could achieve the purifying effect on CO_x , but TD could not.

Purifying Effect at Different UV Intensities

To examine the impact of UV radiation on purifying performance, the relationship between purifying rate and

UV intensity was investigated over time on the PTD, STD, and TD micro surfacing. The test results are plotted in **Figure 7B**.

It was shown that the pollutant purifying performance of purifying micro surfacing could be greatly promoted by UV light intensity, especially for the effect on NO_x . The enhancing effect of UV intensity was noticeable on purifying performances on NO_x of all types of micro surfacing. When the UV intensity was 10 W/m^2 , a turning point emerged in the curves showing the purifying effect on NO_x . When the UV intensity exceeded 10 W/m^2 , the raising speed of the curve began to slow down, which meant that the dependence of purification on UV radiation started to weaken. For CO_x , the purifying rates of PTD and STD micro surfacing subjected



to the increase of UV intensity showed a similar trend that followed the degradation curve of NO_x. However, the TD micro surfacing had no significant degradation effect on CO_x and the purifying effect was around 3%, even if the UV light intensity increased.

With the addition of modified pyrite and specularite, the NO_x and CO_x degradation rates of PTD and STD micro surfacing had been significantly improved compared to TD, while the UV intensity increased. The purifying effects of PTD and STD on NO_x and CO_x reached ~40 and 30%, respectively. The improvement of the purifying effect might be led by the thermoelectric properties of modified pyrite and specularite. In addition, the increasing temperature of the specimen led by UV radiation might also activate the thermoelectric properties, which enhanced the purifying effect of pyrite and specularite.

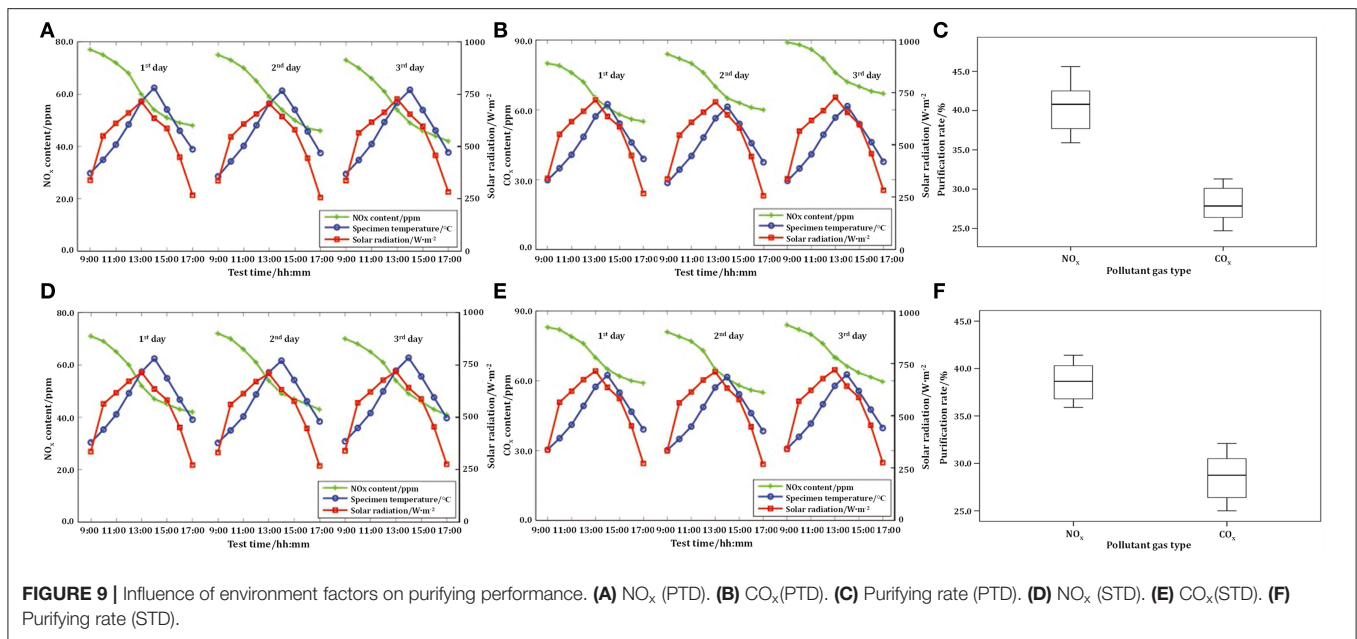
Purifying Effect at Different Specimen Temperatures

The purification testing results of micro surfacing subjected to different specimen temperatures are presented in **Figure 7C**. As shown in **Figure 7C**, the increasing specimen temperature

would enhance the NO_x and CO_x degradation rates of PTD, STD, and TD micro surfacing. For NO_x, the degradation rate curves of three micro surfacing showed a similarly increasing trend, while the gap between the hybrid micro surfacing and TD micro surfacing became larger with the increase of specimen temperature. This experimental conclusion was in line with that of the purifying effect at different UV intensities. For CO_x, PTD, and STD micro surfacing presented superior purifying performances, which could reach almost 40%. However, the TD micro surfacing had a limited removal effect on CO_x when temperature rose.

Purifying Effect at Different Pollutant Concentrations

Considering the variation of pollutant concentrations in an application environment (a highway, tunnel, bridge, etc.), the pollutant concentration would be an important factor among different influencing elements of purifying performance. The testing results at different pollutant concentrations are presented in the **Figure 7D**. The pollutant concentration had a noticeable negative linear effect on the degradation performance of purifying micro surfacing. This might be because that a



higher pollutant concentration would promote the conversion rate reaching its limit, and the overall purification effect then began to decrease. The NO_x and CO_x degradation rates of PTD and STD micro surfacing could still be over 40 and 30%, respectively, higher than that of TD micro surfacing.

Field Testing Results at Complex Environmental Conditions

The varying curves of pollutant gas concentration over the whole 10-day field testing period are plotted in Figure 8.

During the 8 h test period (9:00–17:00) of the 10 selected days, the NO_x and CO_x concentration decreased gradually. The initial value of the pollutant was within the specific range of the experiment condition described before. No obvious outliers were found among the experimental data. It could be calculated that the purifying effect of PTD on NO_x and CO_x were ~40 and 35 ppm, respectively. Concerning STD, the purifying effects on NO_x and CO_x were about 34 and 32 ppm. Analyzing the median variation of pollutant concentration, there was a turning point that appeared at 13:00. For more accurate analysis, the experimental data obtained from three consecutive days, whose environmental parameters (solar radiation, temperature, etc.) were approximately identical, were chosen for the following analysis.

The variations of pollutant concentration, solar radiation intensity, and specimen temperature are presented in Figures 9A,B,D,E. The same trend of variation curves was observed for all the experimental results. Both NO_x and CO_x concentration showed an obvious decreasing trend along with the variation of environmental factors. This indicated that PTD and STD micro surfacing had

noticeable purifying effects on NO_x and CO_x in the field test. The curve of pollutant concentration changed in an approximate linear trend, as solar radiation intensity and specimen increased. When the solar radiation intensity reached its peak value, a turning point appeared in the pollutant concentration curve. The curve slope began decreasing and the degradation speed started to slow down. This observation testified that the UV radiation was the main parameter influencing the purifying effect of purifying micro surfacing, which was consistent with the results of laboratory experiments.

The purification rates of PTD and STD micro surfacing are plotted in Figures 9C,F. For PTD micro surfacing, the data of the NO_x purifying rate mainly ranged between 35 and 45%. The median of these data was 41% and the upper quartile and lower quartile were 42 and 38%, respectively. The range of CO_x purifying data was from 25 to 30% and the CO_x purifying rate of PTD micro surfacing was around 27%. For STD micro surfacing, the NO_x and CO_x purification rates of STD micro surfacing were ~38 and 28%, respectively.

CONCLUSIONS

This paper discussed the preparation and measurement of the purifying properties of two new hybrid pavement micro surfaces containing titanium dioxide, pyrite, and specularite. The pyrite and specularite were selected as the auxiliary functional materials and modified by using two modifying agents to inspire their purifying potentials. The purifying effects of micro surfacing on NO_x and CO_x were investigated in laboratory and field tests. The purifying effects at different atmospheric pressure, UV intensity, temperature, and pollutant concentration were monitored

and investigated. The major conclusions from this study are shown as following:

- With the addition of pyrite and specularite, the PTD and STD micro surfacing had noticeable purification effects on NO_x and CO_x, while the TD micro surfacing was only effective for the degradation of NO_x.
- The increase of UV intensity and ambient temperature would improve the purifying effect of PTD and STD micro surfacing on NO_x and CO_x.
- High pollutant concentration could lead to the conversion rate reaching its saturation limit and thus decrease the overall purification rates.
- The PTD and STD micro surfacing demonstrated a noticeable purifying performance on NO_x and CO_x in the field test when subjected to complex environmental factors, whose results were consistent with that of the laboratory test.

This paper provides new solutions to develop environmentally friendly pavement materials with superior exhaust purifying performances. Future work will focus on further studying the purifying performance of purifying micro surfacing within enclosed environments and the durability of the purifying function.

REFERENCES

- Amato, F., Cassee, F. R., van der Gon, H. A. D., Gehrig, R., Gustafsson, M., Hafner, W., et al. (2014). Urban air quality: the challenge of traffic non-exhaust emissions. *J. Hazard. Mater.* 275, 31–36. doi: 10.1016/j.jhazmat.2014.04.053
- ASTM D113 (2007). *Standard Test Method for Ductility of Bituminous*. West Conshohocken, PA: ASTM International.
- ASTM D2419 (2014). *Standard Test Method for Sand Equivalent Value of Soils and Fine Aggregate*. West Conshohocken, PA: ASTM International.
- ASTM D244 (2017). *Standard Test Methods and Practices for Emulsified Asphalts*. West Conshohocken, PA: ASTM International.
- ASTM D36 (2014). *Test Method for Softening Point of Bitumen (Ring-and-Ball Apparatus)*. West Conshohocken, PA: ASTM International.
- ASTM D5 (2013). *Standard Test Method for Penetration of Bituminous Materials*. West Conshohocken, PA: ASTM International.
- ASTM D6930 (2010). *Standard Test Method for Settlement and Storage Stability of Emulsified Asphalts*. West Conshohocken, PA: ASTM International.
- ASTM D6997 (2004). *Standard Test Method for Distillation of Emulsified Asphalt*. West Conshohocken, PA: ASTM International.
- ASTM E303 (2013). *Standard Test Method for Measuring Surface Frictional Properties Using the British Pendulum Tester*. West Conshohocken, PA: ASTM International.
- ASTM ED3910 (2011). *Standard Practices for Design, Testing, and Construction of Slurry Seal*. West Conshohocken, PA: ASTM International.
- Beale, A. M., Gao, F., Lezcano-Gonzalez, I., Peden, C. H., and Szanyi, J. (2015). Recent advances in automotive catalysis for NO_x emission control by small-pore microporous materials. *Chem. Soc. Rev.* 44, 7371–7405. doi: 10.1039/C5CS00108K
- Brijesh, P., and Sreedhara, S. (2013). Exhaust emissions and its control methods in compression ignition engines: a review. *Int. J. Auto. Tech-Kor.* 14, 195–206. doi: 10.1007/s12239-013-0022-2
- Cai, X., Wu, K., and Huang, W. (2020). Study on the optimal compaction effort of asphalt mixture based on the distribution of contact points of coarse aggregates. *Road Mater. Pavement.* 2020, 1–22. doi: 10.1080/14680629.2019.1710238
- Çay, Y., Korkmaz, I., Çiçek, A., and Kara, F. (2013). Prediction of engine performance and exhaust emissions for gasoline and methanol using artificial neural network. *Energy* 50, 177–186. doi: 10.1016/j.energy.2012.10.052

DATA AVAILABILITY STATEMENT

All datasets generated for this study are included in the article/supplementary material.

AUTHOR CONTRIBUTIONS

XS: data curation. XS and XQ: formal analysis. XS: investigation. XS and ZL: methodology. XS: writing – original draft. DZ, ZL, and YY: writing – review and editing. All authors: contributed to the article and approved the submitted version.

FUNDING

This paper describes research activities mainly requested and sponsored by the Shanxi Transportation Holding Group Co., Ltd. under grant number 19-JKKJ-20, by the Guangdong Provincial Department of Education under grant number 2018KQNCX067, by the National Natural Science Foundation of China under grant number 51908130, and by the Foundation Committee of basic and applied basic research of Guangdong Province under grant number 2019A1515110348.

- Chen, Q., Wang, C., Qiao, Z., and Guo, T. (2020). Graphene/tourmaline composites as a filler of hot mix asphalt mixture: preparation and properties. *J. Construct. Build. Mater.* 239:117859. doi: 10.1016/j.conbuildmat.2019.117859
- Fattah, I. R., Masjuki, H. H., Liaquat, A. M., Ramli, R., Kalam, M. A., and Riazuddin, V. N. (2013). Impact of various biodiesel fuels obtained from edible and non-edible oils on engine exhaust gas and noise emissions. *Renew. Sust. Energ. Rev.* 18, 552–567. doi: 10.1016/j.rser.2012.10.036
- Goel, R., and Guttikunda, S. K. (2015). Evolution of on-road vehicle exhaust emissions in Delhi. *Atmos Environ.* 105, 78–90. doi: 10.1016/j.atmosenv.2015.01.045
- Habib, K., and Wenzel, H. (2014). Exploring rare earths supply constraints for the emerging clean energy technologies and the role of recycling. *J. Clean. Prod.* 84, 348–359. doi: 10.1016/j.jclepro.2014.04.035
- Hirata, H. (2014). Recent research progress in automotive exhaust gas purification catalyst. *Catal. Surv. Asia.* 18, 128–133. doi: 10.1007/s10563-014-9170-2
- Hofmann, G., Rochet, A., Ogel, E., Casapu, M., Ritter, S., Ogurreck, M., et al. (2015). Aging of a Pt/Al₂O₃ exhaust gas catalyst monitored by quasi in situ X-ray micro computed tomography. *RSC. Adv.* 5, 6893–6905. doi: 10.1039/C4RA14007A
- Huang, W., Cai, X., Li, X., Cui, W., and Wu, K. (2020). Influence of nominal maximum aggregate size and aggregate gradation on pore characteristics of porous asphalt concrete. *Materials* 13:1355. doi: 10.3390/ma13061355
- Huang, W., Wang, H., Yin, Y., Zhang, X., and Yuan, J. (2019). Microstructural modeling of rheological mechanical response for asphalt mixture using an image-based finite element approach. *Materials* 12:2041. doi: 10.3390/ma12132041
- Hwang, J. (2013). Sustainability study of hydrogen pathways for fuel cell vehicle applications. *Renew. Sust. Energ. Rev.* 19, 220–229. doi: 10.1016/j.rser.2012.11.033
- ISO 10498 (2004). *Ambient Air–Determination of Sulfur Dioxide–Ultraviolet Fluorescence Method*. Geneva.
- ISO 22197-1 (2007). *Fine Ceramics (Advanced Ceramics, Advanced Technical Ceramics)–Test Method for Air Purification Performance of Semiconducting Photocatalytic Materials–Part 1: Removal of Nitric Oxide*. Geneva.
- ISO 4224 (2000). *Ambient Air–Determination of Carbon Monoxide–Non-Dispersive Infrared Spectrometric Method*. Geneva.

- ISO 7996 (1985). *Ambient air–Determination of the Mass Concentration of Nitrogen Oxides–Chemiluminescence Method*. Geneva.
- ISSA TB-147 (2000). *Multilayer Loaded Wheel Test. International Slurry Surfacing Association*. Annapolis.
- Jhala, K., Natarajan, B., Pahwa, A., and Erickson, L. (2014). “Coordinated electric vehicle charging solutions using renewable energy sources,” in *2014 IEEE Symposium on Computational Intelligence Applications in Smart Grid (CIASG)* (Geneva: IEEE), 1–6. doi: 10.1109/CIASG.2014.7011549
- JTG E60 (2008). *Field Test Methods of Subgrade and Pavement for Highway Engineering*. Beijing: Research Institute of Highway Ministry of Transport.
- Kimble, C., and Wang, H. (2013). China’s new energy vehicles: value and innovation. *J. Business Strategy* 34, 13–20. doi: 10.1108/02756661311310413
- Labarraque, G., Oster, C., Fiscicaro, P., Meyer, C., Vogl, J., Noordmann, J., et al. (2015). Reference measurement procedures for the quantification of platinum-group elements (PGEs) from automotive exhaust emissions. *Int. J. Environ. An. Ch.* 95, 777–789. doi: 10.1080/03067319.2015.1058931
- Lan, L., Chen, S., Cao, Y., Wang, S., Wu, Q., Zhou, Y., et al. (2015). Promotion of CeO₂–ZrO₂–Al₂O₃ composite by selective doping with barium and its supported Pd-only three-way catalyst. *J. Mol. Catal. A-Chem.* 410, 100–109. doi: 10.1016/j.molcata.2015.09.016
- Liu, H., and Liang, D. (2013). A review of clean energy innovation and technology transfer in China. *Renew. Sust. Energ. Rev.* 18, 486–498. doi: 10.1016/j.rser.2012.10.041
- Liu, K., Li, Y., Wang, F., Xie, H., Pang, H., and Bai, H. (2019a). Analytical and model studies on behavior of rigid polyurethane composite aggregate under compression. *J. Mater. Civil Eng.* 31:04019007. doi: 10.1061/(ASCE)MT.1943-5533.0002641
- Liu, K., Liang, W., Ren, F., Ren, J., Wang, F., and Ding, H. (2019b). The study on compressive mechanical properties of rigid polyurethane grout materials with different densities. *Construct. Build. Mater.* 206, 270–278. doi: 10.1016/j.conbuildmat.2019.02.012
- Miyamoto, A., Nagumo, R., Suzuki, A., Miura, R., Tsuboi, H., Hatakeyama, N., et al. (2012). *Electronic and Atomic Roles of Cordierite Substrate in Sintering of Washcoated Catalysts for Automotive Exhaust Gas Emissions Control: Multi-Scale Computational Chemistry Approach Based on Ultra-Accelerated Quantum Chemical Molecular Dynamics Method (No. 2012-01-1292)*. SAE Technical Paper. Geneva. doi: 10.4271/2012-01-1292
- Opitz, B., Drochner, A., Vogel, H., and Votsmeier, M. (2014). An experimental and simulation study on the cold start behaviour of particulate filters with wall integrated three-way catalyst. *Appl. Catal. B-Environ.* 144, 203–215. doi: 10.1016/j.apcatb.2013.06.035
- Ouyang, J., Han, B. G., Cao, Y., Zhou, W. J., Li, W. G., and Surendra, P. S. (2016). The role and interaction of superplasticizer and emulsifier in fresh cement asphalt emulsion paste through rheology study. *J. Construct. Build. Mater.* 125, 643–653. doi: 10.1016/j.conbuildmat.2016.08.085
- Ouyang, J., Hu, L. J., Li, H. Y., and Han, B. G. (2018a). Effect of cement on the demulsifying behavior of over-stabilized asphalt emulsion during mixing. *J. Construct. Build. Mater.* 177, 252–260. doi: 10.1016/j.conbuildmat.2018.05.141
- Ouyang, J., Pan, B., Xu, W., and Hu, L. (2019). Effect of water content on volumetric and mechanical properties of cement bitumen emulsion mixture. *J. Mater. Civil Eng.* 31:04019085. doi: 10.1061/(ASCE)MT.1943-5533.00027361
- Ouyang, J., Yang, W., Chen, J., and Han, B. (2020). Effect of superplasticizer and wetting agent on pavement properties of cold recycled mixture with bitumen emulsion and cement. *J. Mater. Civil Eng.* 32:04020136. doi: 10.1061/(ASCE)MT.1943-5533.0003194
- Ouyang, J., Zhao, J., and Tan, Y. (2018b). Modelling the mechanical properties of cement asphalt emulsion mortar with different asphalt to cement ratio and temperature. *J. Mater. Civil Eng.* 30:04018263. doi: 10.1061/(ASCE)MT.1943-5533.0002480
- Park, C. W., Lee, S. Y., Yi, U. H., and Lee, J. H. (2015). Emission reduction characteristics of three-way catalyst with engine operating condition change in an ultra-lean gasoline direct injection engine. *Trans. Korean Soc. Mech. Eng. B* 39, 727–734. doi: 10.3795/KSME-B.2015.39.9.727
- Peng, B., Cai, C., Yin, G., Li, W., and Zhan, Y. (2015). Evaluation system for CO₂ emission of hot asphalt mixture. *J. Traffic Transport. Eng.* 2, 116–124. doi: 10.1016/j.jtte.2015.02.005
- Pinzi, S., Rounce, P., Herreros, J. M., Tsolakis, A., and Dorado, M. P. (2013). The effect of biodiesel fatty acid composition on combustion and diesel engine exhaust emissions. *Fuel* 104, 170–182. doi: 10.1016/j.fuel.2012.08.056
- Qin, X., Shen, A., Guo, Y., Li, Z., and Lv, Z. (2018). Characterization of asphalt mastics reinforced with basalt fibers. *J. Construct. Build. Mater.* 159, 508–516. doi: 10.1016/j.conbuildmat.2017.11.012
- Rêgo, A. T., Hanriot, S. M., Oliveira, A. F., Brito, P., and Rêgo, T. F. U. (2014). Automotive exhaust gas flow control for an ammonia–water absorption refrigeration system. *Appl. Therm. Eng.* 64, 101–107. doi: 10.1016/j.applthermaleng.2013.12.018
- Schmeisser, V., Weibel, M., Hernando, L. S., Nova, I., Tronconi, E., and Ruggeri, M. P. (2013). Cold start effect phenomena over zeolite scr catalysts for exhaust gas aftertreatment. *SAE Int. J. Commercial Vehicles* 6, 190–199. doi: 10.4271/2013-01-1064
- Sprouse, I. I. C., and Depcik, C. (2013). Review of organic Rankine cycles for internal combustion engine exhaust waste heat recovery. *Appl. Therm. Eng.* 51, 711–722. doi: 10.1016/j.applthermaleng.2012.10.017
- Sun, X., Qin, X., Li, S., Zou, C., Wang, C., and Wang, X. (2018). Characterization of thermal insulating micro-surfacing modified by inorganic insulating material. *J. Construct. Build. Mater.* 175, 296–306. doi: 10.1016/j.conbuildmat.2018.04.170
- Sun, X., Qin, X., Liu, Z., Yin, Y., Jiang, S., and Wang, X. (2020a). Applying feasibility analysis and catalytic purifying potential of novel modifying agent used in asphalt pavement materials. *J. Construct. Build. Mater.* 245:118467. doi: 10.1016/j.conbuildmat.2020.118467
- Sun, X., Qin, X., Liu, Z., Yin, Y., Zou, C., and Jiang, S. (2020b). New preparation method of bitumen samples for UV aging behavior investigation. *J. Construct. Build. Mater.* 233:117278. doi: 10.1016/j.conbuildmat.2019.117278
- Tong, H., Rappold, A. G., Caughey, M., Hinderliter, A. L., Graff, D. W., Berntsen, J. H., et al. (2014). Cardiovascular effects caused by increasing concentrations of diesel exhaust in middle-aged healthy GSTM1 null human volunteers. *Inhal. Toxicol.* 26, 319–326. doi: 10.3109/08958378.2014.889257
- Wang, C., Chen, Q., Guo, T., and Li, Q. (2020). Environmental effects and enhancement mechanism of graphene/tourmaline composites. *J. Clean Prod.* 262:121313. doi: 10.1016/j.jclepro.2020.121313
- Wang, D., Zamel, N., Jiao, K., Zhou, Y., Yu, S., Du, Q., et al. (2013). Life cycle analysis of internal combustion engine, electric and fuel cell vehicles for China. *Energy* 59, 402–412. doi: 10.1016/j.energy.2013.07.035
- Wei, Z., Niu, H., and Ji, Y. (2009). Simultaneous removal of SO₂ and NO_x by microwave with potassium permanganate over zeolite. *Fuel. Process. Technol.* 90, 324–329. doi: 10.1016/j.fuproc.2008.09.005
- Yan, F., Winijkul, E., Bond, T. C., and Streets, D. G. (2014). Global emission projections of particulate matter (PM): II. uncertainty analyses of on-road vehicle exhaust emissions. *Atmos Environ.* 87, 189–199. doi: 10.1016/j.atmosenv.2014.01.045
- Yu, H., Leng, Z., Zhou, Z., Shih, K., Xiao, F., and Gao, Z. (2017). Optimization of preparation procedure of liquid warm mix additive modified asphalt rubber. *J. Clean. Prod.* 141, 336–345. doi: 10.1016/j.jclepro.2016.09.043
- Yu, H., Zhu, Z., Leng, Z., Wu, C., Zhang, Z., Wang, D., et al. (2020). Effect of mixing sequence on asphalt mixtures containing waste tire rubber and warm mix surfactants. *J. Clean. Prod.* 246:119008. doi: 10.1016/j.jclepro.2019.119008
- Yu, H., Zhu, Z., Zhang, Z., Yu, J., Oeser, M., and Wang, D. (2019). Recycling waste packaging tape into bituminous mixtures towards enhanced mechanical properties and environmental benefits. *J. Clean. Prod.* 229, 22–31. doi: 10.1016/j.jclepro.2019.04.049
- Zeng, F., and Hohn, K. L. (2016). Modeling of three-way catalytic converter performance with exhaust mixture from natural gas-fueled engines. *Appl. Catal. B-Environ.* 182, 570–579. doi: 10.1016/j.apcatb.2015.10.004

Conflict of Interest: The authors declare that this study received funding from Shanxi Transportation Holding Group Co., Ltd. The funder was not involved in the study design, collection, analysis, interpretation of data, the writing of this article, or the decision to submit it for publication.

Copyright © 2020 Sun, Liu, Qin, Zeng and Yin. This is an open-access article distributed under the terms of the Creative Commons Attribution License (CC BY). The use, distribution or reproduction in other forums is permitted, provided the original author(s) and the copyright owner(s) are credited and that the original publication in this journal is cited, in accordance with accepted academic practice. No use, distribution or reproduction is permitted which does not comply with these terms.